HHS Public Access

Author manuscript

J Pathol. Author manuscript; available in PMC 2021 June 18.

Published in final edited form as:

J Pathol. 2019 December ; 249(4): 435–446. doi:10.1002/path.5330.

Diabetes induces myeloid bias in bone marrow progenitors associated with enhanced wound macrophage accumulation and impaired healing

Pijus K Barman, **Norifumi Urao**, **Timothy J Koh***

Center for Wound Healing and Tissue Regeneration, Department of Kinesiology and Nutrition, University of Illinois at Chicago, Chicago, IL, USA

Abstract

Diabetes induces dysregulation throughout the spectrum of myeloid lineage cells from progenitors to terminally differentiated cells. Another complication of diabetes is persistent inflammation, including prolonged accumulation of macrophages, which contributes to impaired wound healing. However, it remains unclear whether diabetes disrupts the response of bone marrow progenitors to peripheral injury and whether such dysregulation leads to sustained inflammation and impaired healing. Here, we demonstrated that diabetic mice (db/db, referred to here as DB) exhibit myeloid lineage bias during homeostasis and following injury. In addition, cells in the LSK (Lin $^{-}$Sca-1^{+}cKit^{+}) population of DB mice are preprogrammed towards myeloid commitment at the transcriptional level, and cultured myeloid progenitors from DB mice produce more monocytes *ex vivo* than their non-diabetic counterparts. We also show via bone marrow transfer between interleukin-1 receptor 1 KO (Il1r1$^{-/-}$) and DB mice that IL-1R1 signaling is likely not involved in myeloid skewing in DB mice. Furthermore, *in vitro* experiments indicated that macrophage colony-stimulating factor receptor signaling is not likely involved in enhanced myeloid transcription factor expression in LSK cells of DB mice. Our findings indicate that myeloid lineage commitment in bone marrow may contribute to increased macrophage numbers observed in diabetic skin wounds, and that strategies to regulate monopoiesis during homeostasis or post-wounding may improve diabetic wound healing.

Keywords

diabetes; wound healing; inflammation; macrophage; myeloid; progenitors; hematopoietic stem and progenitor cells; M-CSF; IL-1; myelopoiesis

*Correspondence to: TJ Koh, University of Illinois at Chicago, Center for Wound Healing and Tissue Regeneration, Department of Kinesiology and Nutrition, 1919 W Taylor Street, Chicago, IL 60612-7246, USA. tjkoh@uic.edu.

Author contributions statement

PKB designed and performed experiments, analyzed and interpreted data, and wrote the manuscript. NU contributed to study design, interpreted data, and reviewed and edited the manuscript. TJK designed the study and wrote the manuscript. TJK is the guarantor of this work and, as such, had full access to all of the data in the study and takes responsibility for the integrity of the data and the accuracy of the data analysis.

Data Availability Statement

The datasets generated during and/or analyzed during the current study are available from the corresponding author upon reasonable request. No applicable resources were generated or analyzed during the current study.

Introduction

Diabetic ulcers are a major health concern with increasing socioeconomic burden [1–3]. Cells of the monocyte/macrophage lineage (Mo/Mp) play important roles in skin wound healing [4–10], but persistent accumulation of inflammatory Mo/Mp contributes to chronic inflammation in poorly healing diabetic wounds [11–15]. Wound Mo/Mp are thought to originate primarily from circulating monocytes, which in turn are supplied by bone marrow (BM) [4,8,9], and we recently reported that skin wounding increases hematopoietic stem and progenitor cell (HSPC) numbers and promotes monocyte expansion in the BM of mice [16]. However, links between diabetes, (dys)regulation of HSPC populations, persistent wound Mo/Mp accumulation, and impaired healing remain to be elucidated.

A number of studies have demonstrated the effects of obesity, hypercholesterolemia, and hyperglycemia on the hematopoietic system [17–26]. For example, hyperglycemia can preprogram HSPCs towards myeloid lineage commitment [21]. Similarly, both diet-induced and genetically modified obese (ob/ob) mice exhibit increased myelopoiesis [17,23–25]. Obesity may also induce epigenetic modifications in HSPCs that bias progeny, leading to increased inflammatory wound Mp phenotypes and impaired skin wound healing [12]. However, much remains to be learned about how diabetes induces dysregulation of HSPC subpopulations and how these alterations influence wound Mp activity and subsequent healing.

In the present study, we provide evidence that enhanced myeloid cell production in type 2 diabetic mice (db/db; hereafter called DB) following skin wounding likely results from alterations in bone marrow progenitors generated during homeostasis and maintained following injury. Diabetic mice exhibited increased proportions of bone marrow myeloid progenitors (MyP) and circulating inflammatory monocytes (Mo) *before* skin wounding, and enhanced myeloid output was maintained following injury, contributing to a greater number of wound Mp. In addition, cells of the LSK ($Lin^{-}Sca\text{-}1^{+}cKit^{+}$) population from diabetic mice appeared to be preprogrammed towards myeloid commitment at the transcriptional level, and cultured MyP from diabetic mice produced more Mo *ex vivo* than their wild-type counterparts. Finally, we showed that interleukin-1 receptor 1 (IL-1R1) and macrophage colony-stimulating factor receptor (M-CSFR) signaling, which are known to induce myelopoiesis in WT HSC [27,28], are likely not involved in myeloid skewing in DB mice.

Materials and methods

Animals

Diabetic db/db (DB) on the BKS background, interleukin-1 receptor 1 knockout mice ($Il1r1^{-/-}$) mice on the C57Bl/6 background, and non-diabetic (ND) C57BL/6 controls were obtained from Jackson Laboratories (Bar Harbor, ME, USA). Our preliminary experiments indicated no differences in bone marrow HSPC populations, wound Mo/Mp populations, or wound healing between C57Bl/6 and BKS control mice; thus, C57Bl/6 mice were used as controls for the present study. Experiments were performed on 8- to 12-week-old mice. All experimental procedures were approved by the Animal Care Committee at the University of Illinois at Chicago.

Excisional skin wounding

Mice were subjected to two excisional skin wounds using an 8 mm biopsy punch as described previously [13,29,30].

Bone marrow transfer

Bone marrow-recipient mice (8- to 10-week-old DB mice) were lethally irradiated using two doses of 5 Gray with 3 h between doses. Bone marrow cells were collected from donor 8- to 10-week-old Il1r1$^{-/-}$ or C57BL/6 wild-type control mice and injected retro-orbitally (5×10^6 cells per mouse in 200 μl of PBS) into recipient mice on day 1 after lethal irradiation. Six weeks later, mice were sacrificed and cells were collected for analysis.

Cell isolation

Cells from excisional skin wounds of mice were dissociated enzymatically [13,30]. For BM cells, femurs were isolated and marrow was flushed out with cold fluorescence-activated cell sorting (FACS) buffer. Splenic cells were prepared by dissociating spleen in FACS buffer and then passing the cell suspension through a 70 μm mesh cell strainer. Peripheral blood was collected in EDTA-containing collection tubes.

Flow cytometry

Details of the antibodies used for flow cytometry are listed in supplementary material, Table S1. For identification of stem cell populations, BM single cells were incubated with biotin-conjugated antibodies targeting the lineage markers CD45R, CD3e, Gr1, TER-119, CD11b, CD4, CD8a, CD19, NK1.1, and CD127, followed by either streptavidin-APC-Cy7, Sca-1-PerCP-Cy5.5, cKit-Alexa Fluor 647, Flk2-BV421, CD150-PE-Dazzle594, and CD48-PE, or streptavidin-APC-Cy7, Sca-1-PerCP-Cy5.5, cKit-Alexa Fluor 647, FcRγ-V450, and CD34-FITC. For identification of myeloid cells in BM, spleen or blood, cells were incubated with antibodies against Ly6G-BV421, CD11b-APC-eFluor 780, CD115-PE, and Ly6C-FITC. For wound myeloid cells, enzymatically dissociated single cells were incubated with Zombie-BV421, CD45-FITC, Ly6G-PE-CF594, CD11b-APC-eFluor780, F4/80-PE, and Ly6C-PerCPCy5.5. To assess surface M-CSFR on HSPCs, BM cells were incubated with biotin-conjugated antibodies targeting lineage markers, followed by streptavidin-APC-Cy7, Sca-1-PerCP-Cy5.5, cKit-Alexa Fluor 647, FcRγ-V450, CD34-FITC, and CD115.

For progenitor sorting, BM cells were enriched for lineage$^-$ cells using EasySep™ Mouse Hematopoietic Progenitor Cell Isolation Kit and following the manufacturer's protocol (Stem Cell Technologies, Vancouver, BC, Canada). Lineage$^-$ cells were then incubated with streptavidin-eFluor450 (to exclude any residual lineage$^+$ cells that had bound biotin-conjugated antibodies to lineage markers but were not depleted during magnetic sorting), Sca-1-PE-Cy7, and cKit-Alexa Fluor 647. For assessing Mo differentiation in culture, differentiated cells were incubated with CD11b-APC-eFluor 780, Ly6C-FITC, and FcRγ-BV421 antibodies. Cell sorting was performed on MoFlo Astrios (Beckman Coulter, Brea, CA, USA) and cell analyses were done using LSR II Fortessa (Becton Dickenson, Franklin Lakes, NJ, USA).

Clonogenic assay

Thirty thousand BM cells were cultured per 30 mm dish in MethoCult™ GF M3534 medium following the manufacturer's protocol (Stem Cell Technologies, Vancouver, BC, Canada) and granulocyte-macrophage colony-forming units (CFU-GM) were counted under a microscope following culture for 9 days.

RT-qPCR

RNA isolation from FACS-sorted LSK or MyP and first-strand cDNA synthesis were accomplished using a Power SYBR Green Cells-to-CT kit. Quantitative PCR was performed using either power SYBR Green PCR Master Mix and custom-designed primers or TaqMan Universal PCR Master Mix or TaqMan Gene Expression Assay primer/probe sets as listed in supplementary material, Table S2. Relative gene expression was determined using the $2^{-\Delta\Delta CT}$ method, using *Actb* as a reference transcript.

Cell culture

Flow-sorted MyP and LSK cells were grown in Stem-Pro34 medium (Thermo Fisher Scientific, Canoga Park, CA, USA) supplemented with penicillin (50 U/ml)/streptomycin (50U/ml) and l-glutamine (2mM), SCF (25ng/ml), and Flt3L (25ng/ml). IL-1β was added at 5 ng/ml and M-CSF at 25 or 100ng/ml.

IL-1β measurement in BM plasma

BM plasma was collected as described previously [16]. IL-1β protein was measured in BM plasma using an ELISA kit following the manufacturer's instructions (R&D Systems, Minneapolis, MN, USA).

Statistics

Results are expressed as mean ± SD. Statistical analyses were performed using Prism 7.0 software (Graph-Pad Inc, San Diego, CA, USA). Data between two groups were compared using two-way ANOVA, and different time points in the same group using one-way ANOVA (Kruskal–Wallis test) in kinetic assays. Two time points or two groups were compared using a *U*-test (Mann-Whitney). Differences between groups were considered significant if $p \leq 0.05$.

Results

Type 2 diabetes (T2D) preprograms HSPCs towards myeloid differentiation at baseline

Previous studies have demonstrated that diet-induced obesity results in an increased frequency of HSPCs in the BM of mice [23]. Hence, we tested whether T2D influences HSPCs in DB mice (Figure 1A and supplementary material, Figure S1A). DB mice had a significantly greater frequency of LSK cells in the BM compared with ND controls (Figure 1B,C). Further analysis of HSPC subsets revealed a statistically non-significant trend ($p=0.09$) for increased frequency of long-term repopulating hematopoietic stem cells (HSC-LT: $Lin^{-}Sca\text{-}1^{+}cKit^{+}Flk2^{-}CD48^{-}CD150^{+}$) and short-term repopulating hematopoietic stem cells (HSC-ST: $Lin^{-}Sca\text{-}1^{+}cKit^{+}Flk2^{-}CD48^{-}CD150^{-}$) in DB mice. In addition, there were

no differences for multipotent progenitors (MPP2: $Lin^{-}Sca\text{-}1^{+}cKit^{+}Flk2^{-}CD48^{+}CD150^{+}$; MPP3: $Lin^{-}Sca\text{-}1^{+}cKit^{+}Flk2^{-}CD48^{+}CD150^{-}$; MPP4: $Lin^{-}Sca\text{-}1^{+}cKit^{+}Flk2^{+}CD150^{-}$) between strains (Figure 1B–D). Differences in the numbers of LSK cells or any other cell type were found not to be statistically significant (supplementary material, Figure S1B,C).

In addition, consistent with earlier studies of different models of obesity and hyperglycemia [21,23], the frequency of MyP ($Lin^{-}Sca\text{-}1^{-}cKit^{+}$) was found to be higher in DB BM than in ND controls (Figure 1B,E and supplementary material, Figure S1D). Interestingly, among all the MyP subsets, only granulocyte macrophage progenitors (GMP: $Lin^{-}Sca\text{-}1^{-}cKit^{+}FcR\gamma hiCD34^{+}$) showed a significantly increased frequency in DB mice. Common myeloid progenitors (CMP: $Lin^{-}Sca\text{-}1^{-}cKit^{+}FcR\gamma loCD34^{+}$) showed a statistically non-significant trend (p=0.09) of increased frequency in DB mice, and megakaryocyte erythrocyte progenitors (MEP: $Lin^{-}Sca\text{-}1^{-}cKit^{+}FcR\gamma loCD34^{-}$) showed nearly identical frequencies in both strains (Figure 1B,E,F and supplementary material, Figure S1D,E). Taken together, we interpret this to support increased myeloid lineage commitment in DB mice at the progenitor level.

Next, we examined whether downstream myeloid cells were altered in DB mice by scoring Ly6Chi Mo ($Ly6G^{-}CD11b^{+}Ly6Chi$) and neutrophils ($Ly6G^{+}$) in peripheral blood, spleen, and BM of DB and ND mice (Figure 1G and supplementary material, Figure S1F,G). DB mice had a significantly higher percentage of both Ly6Chi Mo and neutrophils in their circulation and spleen. In contrast, neither Mo nor neutrophils were found to be different in the BM between strains (Figure 1G and supplementary material, Figure S1F,G).

To directly assess HSPC differentiation potential, we counted colony-forming units (CFU) after 9 days of whole BM culture in a methylcellulose medium that supported HSPC differentiation only into CFU-GM. There was a remarkably higher number of CFU-GM in the culture derived from DB BM (Figure 1H,I). These data are consistent with our flow cytometry analyses showing increased myeloid commitment in DB mice at the progenitor level (Figure 1A–F).

We measured relative levels of mRNA expression for critical transcription factors (TFs) and growth factor receptors associated with myeloid differentiation in LSK cells isolated from DB and ND BM. We found that the levels of mRNA for the TFs Spi1, Cebpa, and Hoxa9 were upregulated in the LSK cells derived from DB compared with ND mice (Figure 2A,B). In addition, DB LSK cells showed upregulated expression of *Csf1r* (colony-stimulating factor 1 receptor) and *Csf2ra* (colony-stimulating factor 2 receptor alpha subunit) (Figure 2B). Furthermore, increased levels of M-CSFR protein were observed on DB LSK cells, as determined by both a higher percentage of cells and the mean fluorescence intensity (MFI) of surface M-CSFR in flow cytometry analyses (Figure 2C,D). Taken together, these data support the hypothesis that stem cells in DB mice may be intrinsically modified towards myeloid lineage commitment by upregulation of critical TFs and receptors associated with myeloid differentiation.

T2D primes MyP to promote myelopoiesis *ex vivo*

We sought to determine whether MyP are also intrinsically modified to produce myeloid cells. Thus, we measured the expression of myeloid-associated TFs in MyP isolated from DB and ND mice (Figure 3A). MyP from DB mice showed significantly higher expression of *Cebpa* and *Hoxa9* compared with ND controls. Surprisingly, *Spi1* expression was found to be downregulated in DB MyP (Figure 3A,B). Examination of surface M-CSFR revealed both higher percentage and MFI of this receptor on MyP in DB mice. Among all the MyP subsets, GMP showed the highest-level expression of M-CSFR in ND mice, whereas MEP showed an almost undetectable level of this receptor (supplementary material, Figure S2A–D).

To test whether T2D alters Mo production by MyP, we isolated MyP from DB and ND mice and monitored their differentiation into myeloid cells in the presence or absence of IL-1β or M-CSF (Figure 3A). As expected, both IL-1β and M-CSF induced MyP differentiation, leading to increased numbers of total cells, Ly6Chi Mo ($CD11b^+Ly6Chi$), and effector myeloid cells ($CD11b^+FcR\gamma^+$) in both DB- and ND-derived cultures (Figure 3C–H). Importantly, cultures derived from DB mice exhibited greater rates of differentiation to Mo in the presence of both IL-1β and M-CSF, despite starting the culture with the same number of MyP (Figure 3C–H). However, the percentages of myeloid populations produced in response to either M-CSF or IL-1β did not differ between DB and ND MyP cultures, indicating that differences in Mo output resulted primarily from increased total cell output (Figure 3C–H). In summary, previous findings of IL-1β- and M-CSF-induced myelopoiesis in HSC [27,28] were recapitulated in MyP in the present study. Furthermore, our results indicate that MyP from DB mice produce more myeloid cells in response to both IL-1β and M-CSF. Taken together, these data support the hypothesis that T2D primes MyP for myelopoiesis upon exposure to IL-1β and M-CSF.

IL-1R1 and M-CSFR signaling likely do not influence myeloid commitment in T2D mice

Our previous studies showed that sustained activity of the NLRP3 inflammasome and the resulting high levels of IL-1β promoted the accumulation of pro-inflammatory wound Mp in DB mice [29,30]. Further, the finding of enhanced IL-1β-mediated myeloid production by DB MyP (Figure 3A–G) led us to study whether myeloid bias in DB mice was due to IL-1R1 signaling. We tested this by determining whether reconstitution of DB BM with IL-1R1 KO ($Il1r1^{-/-}$) reduces HSPC and Mo cellularity in recipient DB mice (Figure 4A and supplementary material, Figure S2E); in these experiments, donor bone marrow showed more than 95% engraftment at 6 weeks after transplantation (supplementary material, Figure S2E). Importantly, transfer of $Il1r1^{-/-}$ and C57BL/6 WT control donor BM to DB recipient mice resulted in no differences in the percentage of any BM HSPC subset between recipient groups (Figure 4B–F). Similarly, Ly6Chi Mo did not show differences in either the BM or the circulation between recipient groups, indicating that loss of IL-1R1 signaling does impact myeloid skewing in DB mice (Figure 4G). When compared with these recipient groups, DB mice that received the same numbers of DB BM cells showed increased total bone marrow cells and a higher proportion of myeloid progenitor subsets, indicating enhanced reconstitution and myeloid lineage skewing (data not shown). This is likely due to the higher proportion of HSCs observed in DB BM compared with ND BM (Figure 1).

Finally, to test whether IL-1β levels are altered in the BM of T2D mice, we measured IL-1β protein in BM plasma of DB and ND mice; the data revealed no difference in IL-1β level between the BM plasma of the two strains (Figure 4H). Taken together, these data indicate that IL-1β/IL-1R1 signaling is likely not responsible for myeloid bias in DB mice.

Previous studies have demonstrated that M-CSF induces myelopoiesis in ND HSCs through PU.1 [27]. Our findings of increased *Csf1r* mRNA expression and M-CSFR surface protein in DB versus ND LSK cells led us to examine whether M-CSFR signaling mediates the increased myeloid TF expression observed in DB LSK cells. We tested this by measuring the mRNA expression of *Spi1* and *Cebpa* in DB 1and ND LSK cultures in the presence or absence of M-CSF (supplementary material, Figure S2F). In contrast to previous data generated in HSCs [27], M-CSF did not increase PU.1 or CEBP-α expression in LSK cultures derived from either of the strains (supplementary material, Figure S2G). Our data indicate that M-CSFR signaling is likely not responsible for enhanced myeloid TF expression in DB LSK cells. However, further study of the possible role of M-CSFR in myeloid skewing in DB mice is warranted.

T2D alters HSPC response to wounding

We recently reported that different BM HSPC subpopulations respond in a cell-type-specific manner to skin wounding [16], and we hypothesized that diabetes may enhance the HSPC response to skin wounding. We performed excisional skin wounding in DB and ND mice and scored HSPC and MyP subsets in BM at different stages of wound healing (Figure 5 and supplementary material, Figure S3). At baseline, there was a statistically non-significant trend of a higher percentage (p=0.09) of HSC-LT in DB compared with ND mice which was significantly higher at day 1 post-wounding. HSC-LT in ND mice appeared to increase more slowly, reaching levels significantly higher than baseline on day 6 post-wounding. The absolute numbers of HSC-LT also trended higher in DB versus ND BM at day 1 post-wounding (Figure 5B and supplementary material, Figure S3A,C). The HSC-ST subset did not exhibit a wound response in either mouse strain; however, the levels of this subset tended to be higher in DB than in ND mice and was significantly higher at day 3 post-wounding (Figure 5C and supplementary material, Figure S3A,D).

Of all the HSPC subsets, the multipotent progenitors MPP2, MPP3, and MPP4, which are downstream of HSCs in the hierarchy of differentiation, were influenced most by skin wounding (Figure 5D–F and supplementary material, Figure S3A,E–G). Both the frequency and the absolute numbers of MPP2, MPP3, and MPP4 started to increase at day 1 and reached their peak at day 3 post-wounding in ND BM. Following this peak, all MPP subsets declined as healing continued, reaching basal levels by day 9 post-wounding. Interestingly, the responses of MPP2 and MPP3, which are committed to myeloid differentiation [31], were slower in DB mice, resulting in a significantly lower frequency and number of these subsets in DB compared with ND BM at day 3 post-wounding (Figure 5D,E and supplementary material, Figure S3E,F). In contrast, MPP4, which is thought to be committed to lymphoid differentiation, followed almost identical kinetics in both strains following skin wounding (Figure 5F and supplementary material, Figure S3G).

We determined whether myeloid progenitors respond to skin wounding in DB and ND mice. There was a gradual decrease in CMP in both DB and ND BM following skin wounding, although DB mice tended to exhibit higher percentages at baseline which became significant at day 3 post-wounding (Figure 5G and supplementary material, Figure S3B,H). In addition, although GMP were not affected by skin wounding in either of the strains, GMP frequency tended to be higher in DB mice throughout the healing process (Figure 5H and supplementary material, Figure S3B,I). Finally, similar to CMP, MEP gradually decreased following wounding, reaching their lowest level at day 6 post-wounding and recovering towards basal levels afterwards in both DB and ND BM, with no difference in MEP between DB and ND BM at any time point post-wounding (Figure 5I and supplementary material, Figure S3B,J). Taken together, our results showed that BM HSPCs respond differentially to skin wounding in DB and ND mice, with most notable differences in HSC-LT and myeloid-committed MPP2 and three subsets.

T2D increases Ly6Chi Mo in the circulation and spleen following skin wounding

Wound Mo/Mp are thought to be derived primarily from circulating Mo, which in turn are supplied by the BM [4,8,9]. Our results showed that skin wounding increases the proportion of Ly6Chi Mo ($Ly6G^{-}CD11b^{+}Ly6Chi$) in the BM of both DB and ND mice at day 3 post-wounding, followed by a decrease towards baseline. However, there was no difference in BM Ly6Chi Mo between DB and ND mice at any time point following wounding (Figure 6A). In addition, both DB and ND mice showed an increase in the proportion of circulating Ly6Chi Mo, which reached a maximum at day 3 post-wounding. Furthermore, although the kinetic pattern of circulating Ly6Chi Mo was similar in DB and ND mice, the proportion of these cells showed a non-significant increase in DB mice at day 1 post-wounding ($p=0.07$) (Figure 6B). We found that the proportion of splenic Ly6Chi Mo was increased at day 3 and remained high until day 6 post-wounding both in ND and in DB mice. Similar to peripheral blood, Ly6Chi Mo tended to be higher in DB spleen post-wounding at day 3 and onward ($p<0.01$, 0.08, and 0.07 at days 3, 6, and 9, respectively) (Figure 6C). Taken together, these results support the notion that skin wounding increases the number of Ly6Chi Mo in the circulation, spleen, and BM of both DB and ND mice, while circulating and splenic Ly6Chi Mo numbers tended to be higher in DB than in ND mice post-wounding.

Delayed wound closure in T2D mice is associated with increased wound Mo/Mp

Consistent with previous findings, the wound closure rate was significantly delayed in DB mice [13] (supplementary material, Figure S4A,B). To determine whether myeloid bias in BM, blood, and spleen of DB mice extends to wound cells, we assessed Mo/Mp subsets in the wounds of DB and ND mice at different time points following wounding (supplementary material, Figure S4C). Both strains exhibited an increase in Ly6Chi Mo (live $CD45^{+}Ly6G^{-}CD11b^{+}F4/80^{-}Ly6Chi$) on day 1 post-wounding, followed by a rapid decline at day 3. Most strikingly, the number of Ly6Chi Mo was found to be significantly higher in DB wounds than in ND counterparts (Figure 6D,E). This early infiltration of Ly6Chi Mo was followed by a notable increase in Ly6Chi Mp (live $CD45^{+}Ly6G^{-}CD11b^{+}F4/80^{+}Ly6Chi$) in DB wounds at day 3 post-wounding, which were significantly elevated compared with ND wounds (Figure 6D,F). At the same time, Ly6Clo Mp (live $CD45^{+}Ly6G^{-}CD11b^{+}F4/80^{+}Ly6Clo$) were increased in both DB and ND wounds at day 3 post-wounding.

Similar to the Ly6Chi Mo and Mp subsets, Ly6Clo Mp numbers were also found to be significantly higher in DB wounds at days 3 and 6 post-wounding (Figure 6D,G). In sum, these findings support the notion that diabetic wounds are infiltrated with higher number of Ly6Chi Mo during early wound healing and this is followed by significantly larger Mp populations in diabetic wounds as the healing continues.

Discussion

We tested the hypothesis that T2D enhances the response of HSPCs and monopoiesis to skin wounding, contributing to chronic inflammation and impaired wound healing. Our results support that skin wounding induces distinct kinetics of HSCs and myeloid-committed MPPs in ND mice and that diabetes dysregulates this process. Consistent with previous reports using obese, insulin-resistant, and hyperglycemic mouse models [12,17,19,21,23], our study demonstrates that T2D induces the programming of HSCs towards the myeloid lineage in DB mice. Importantly, our data indicate that myeloid skewing of diabetic stem cells is associated with elevated expression of TFs and receptors associated with myeloid commitment. We also show that diabetic MyP possess higher differentiation potential and that increased accumulation of wound Mp in DB mice is associated with elevated Ly6Chi Mo in the circulation and spleen both at the steady state and after skin wounding. Furthermore, our data support the hypothesis that IL-1R1 signaling is likely not responsible for myeloid skewing in DB mice.

Blood cells are produced in a well-regulated hierarchical process of HSPC differentiation during homeostasis [32]. However, this process appears to be altered during emergency need of myeloid cells, as in the case of injury or from inflammatory stimuli [33,34]. The present study addressed whether skin wounding influenced HSPCs and Mo, and whether the pre-existing systemic inflammation present in T2D enhances this response [35–38]. Our results showed that HSC-LT cells are increased in the BM of DB mice during early wound healing. Moreover, to our surprise, wound-induced increases in myeloid-committed MPP2 and MPP3 observed in ND mice were blunted in DB mice. The reason behind the differential responses of diabetic MPPs to skin wounding remains to be elucidated; however, one potential explanation for the lack of MPP2/3 increase in DB BM is that the MPP2/3 pool is used rapidly in DB BM, producing more Mo, whereas the MPP2/3 turnover rate is slower in ND BM, leading to the higher MPP2/3 pool observed in ND BM during early wound healing. We also speculate that wound-induced increases in MPP2 and MPP3 might be tissue regenerative responses in ND mice that are abrogated in diabetic settings. The mechanisms underlying these differences and their downstream consequences require further investigation.

Persistently greater numbers of Mp in diabetic wounds raised the question of whether skin wounding-induced Mo expansion is enhanced in T2D mice [11–15]. Our results show that despite the increased MyP frequency in T2D mice and their greater ability to produce myeloid cells, wound-induced Mo expansion was not enhanced in the BM of DB compared with ND mice. However, the number of Ly6Chi Mo was elevated both in peripheral blood and in the spleen, both at steady state and post-wounding, coinciding with increased wound Mp in DB mice. Thus, the greater number of Mp in diabetic wounds could be the result of

increased monopoiesis in diabetic mice along with elevated mobilization to blood and eventually wound Mo/Mp. Taken together, these data support a hypothesis that a higher basal pool of MyP with higher differential potential may induce Mp dysregulation in diabetic wounds.

Finally, consistent with the well-established role of PU.1 in myeloid lineage commitment [39,40], our results showed that myeloid bias in DB mice is associated with higher PU.1 expression in LSK cells. Further, we showed directly that diabetic MyP produce more myeloid cells in the presence of IL-1β and M-CSF, which have been shown to promote myelopoiesis through PU.1 [27,28]. We speculated that IL-1β and M-CSF may promote myelopoiesis inT2D via PU.1, leading to increased wound Mp in diabetic wounds. However, transfer of $Il1r^{-/-}$ BM to DB mice showed that IL-1R1 signaling is likely not involved in myeloid skewing in DB mice. In addition, *in vitro* experiments indicated that M-CSFR signaling is likely not involved in enhanced myeloid TF expression in LSK cells of DB mice. Further investigation into the mechanisms underlying increased myelopoiesis in diabetes may provide insight into strategies towards the regulation of Mo/Mp in diabetic wounds.

In conclusion, our data indicate that a higher basal pool of MyP along with higher differentiation potential in DB mice may contribute to a heightened Mo/Mp response in skin wounds that contributes to impaired healing in diabetic mice.

Supplementary Material

Refer to Web version on PubMed Central for supplementary material.

Acknowledgements

This work was supported by a grant from the National Institutes of Health (R01GM092850) to TJK. We would also like to thank Dr Giamila Fantuzzi for her input on experimental design and on aspects of presentation of this article.

References

1. Driver VR, Fabbi M, Lavery LA, et al. The costs of diabetic foot: the economic case for the limb salvage team. J Vasc Surg 2010; 52: 17S–22S. [PubMed: 20804928]
2. Gregg EW, Li Y, Wang J, et al. Changes in diabetes-related complications in the United States, 1990–2010. N Engl J Med 2014; 370: 1514–1523. [PubMed: 24738668]
3. Rice JB, Desai U, Cummings AK, et al. Burden of diabetic foot ulcers for Medicare and private insurers. Diabetes Care 2014; 37: 651–658. [PubMed: 24186882]
4. Ishida Y, Gao JL, Murphy PM. Chemokine receptor CX3CR1 mediates skin wound healing by promoting macrophage and fibroblast accumulation and function. J Immunol 2008; 180: 569–579. [PubMed: 18097059]
5. Koh TJ, DiPietro LA. Inflammation and wound healing: the role of the macrophage. Expert Rev Mol Med 2011; 13: e23. [PubMed: 21740602]
6. Lucas T, Waisman A, Ranjan R, et al. Differential roles of macrophages in diverse phases of skin repair. J Immunol 2010; 184: 3964–3977. [PubMed: 20176743]
7. Mirza R, DiPietro LA, Koh TJ. Selective and specific macrophage ablation is detrimental to wound healing in mice. Am J Pathol 2009; 175: 2454–2462. [PubMed: 19850888]
8. Rodero MP, Licata F, Poupel L, et al. *In vivo* imaging reveals a pioneer wave of monocyte recruitment into mouse skin wounds. PLoS One 2014; 9: e108212. [PubMed: 25272047]

9. Willenborg S, Lucas T, van Loo G, et al. CCR2 recruits an inflammatory macrophage subpopulation critical for angiogenesis in tissue repair. Blood 2012; 120: 613–625. [PubMed: 22577176]
10. Wynn TA, Vannella KM. Macrophages in tissue repair, regeneration, and fibrosis. Immunity 2016; 44: 450–462. [PubMed: 26982353]
11. Bannon P, Wood S, Restivo T, et al. Diabetes induces stable intrinsic changes to myeloid cells that contribute to chronic inflammation during wound healing in mice. Dis Model Mech 2013; 6: 1434–1447. [PubMed: 24057002]
12. Gallagher KA, Joshi A, Carson WF, et al. Epigenetic changes in bone marrow progenitor cells influence the inflammatory phenotype and alter wound healing in type 2 diabetes. Diabetes 2015; 64: 1420–1430. [PubMed: 25368099]
13. Mirza R, Koh TJ. Dysregulation of monocyte/macrophage phenotype in wounds of diabetic mice. Cytokine 2011; 56: 256–264. [PubMed: 21803601]
14. Boniakowski AE, Kimball AS, Jacobs BN, et al. Macrophage-mediated inflammation in normal and diabetic wound healing. J Immunol 2017; 199: 17–24. [PubMed: 28630109]
15. Kimball A, Schaller M, Joshi A, et al. Ly6C^{Hi} blood monocyte/macrophage drive chronic inflammation and impair wound healing in diabetes mellitus. Arterioscler Thromb Vasc Biol 2018; 38: 1102–1114. [PubMed: 29496661]
16. Barman PK, Pang J, Urao N, et al. Skin wounding-induced monocyte expansion in mice is not abrogated by IL-1 receptor 1 deficiency. J Immunol 2019; 202: 2720–2727. [PubMed: 30910860]
17. Adler BJ, Green DE, Pagnotti GM, et al. High fat diet rapidly suppresses B lymphopoiesis by disrupting the supportive capacity of the bone marrow niche. PLoS One 2014; 9: e90639. [PubMed: 24595332]
18. Adler BJ, Kaushansky K, Rubin CT. Obesity-driven disruption of haematopoiesis and the bone marrow niche. Nat Rev Endocrinol 2014; 10: 737–748. [PubMed: 25311396]
19. Claycombe K, King LE, Fraker PJ. A role for leptin in sustaining lymphopoiesis and myelopoiesis. Proc Natl Acad Sci U S A 2008; 105: 2017–2021. [PubMed: 18250302]
20. Mihaylova MM, Sabatini DM, Yilmaz OH. Dietary and metabolic control of stem cell function in physiology and cancer. Cell Stem Cell 2014; 14: 292–305. [PubMed: 24607404]
21. Nagareddy PR, Murphy AJ, Stirzaker RA, et al. Hyperglycemia promotes myelopoiesis and impairs the resolution of atherosclerosis. Cell Metab 2013; 17: 695–708. [PubMed: 23663738]
22. Rodrigues M, Wong VW, Rennert RC, et al. Progenitor cell dysfunctions underlie some diabetic complications. Am J Pathol 2015; 185: 2607–2618. [PubMed: 26079815]
23. Singer K, DelProposto J, Morris DL, et al. Diet-induced obesity promotes myelopoiesis in hematopoietic stem cells. Mol Metab 2014; 3: 664–675. [PubMed: 25161889]
24. Trottier MD, Naaz A, Li Y, et al. Enhancement of hematopoiesis and lymphopoiesis in diet-induced obese mice. Proc Natl Acad Sci U S A 2012; 109: 7622–7629. [PubMed: 22538809]
25. van den Berg SM, Seijkens TT, Kusters PJ, et al. Diet-induced obesity in mice diminishes hematopoietic stem and progenitor cells in the bone marrow. FASEB J 2016; 30: 1779–1788. [PubMed: 26813974]
26. Lee JM, Govindarajah V, Goddard B, et al. Obesity alters the long-term fitness of the hematopoietic stem cell compartment through modulation of Gfi1 expression. J Exp Med 2018; 215: 627–644. [PubMed: 29282250]
27. Mossadegh-Keller N, Sarrazin S, Kandalla PK, et al. M-CSF instructs myeloid lineage fate in single haematopoietic stem cells. Nature 2013; 497: 239–243. [PubMed: 23575636]
28. Pietras EM, Mirantes-Barbeito C, Fong S, et al. Chronic interleukin-1 exposure drives haematopoietic stem cells towards precocious myeloid differentiation at the expense of self-renewal. Nat Cell Biol 2016; 18: 607–618. [PubMed: 27111842]
29. Mirza RE, Fang MM, Ennis WJ, et al. Blocking interleukin-1β induces a healing-associated wound macrophage phenotype and improves healing in type 2 diabetes. Diabetes 2013; 62: 2579–2587. [PubMed: 23493576]
30. Mirza RE, Fang MM, Weinheimer-Haus EM, et al. Sustained inflammasome activity in macrophages impairs wound healing in type 2 diabetic humans and mice. Diabetes 2014; 63: 1103–1114. [PubMed: 24194505]

31. Pietras EM, Reynaud D, Kang YA, et al. Functionally distinct subsets of lineage-biased multipotent progenitors control blood production in normal and regenerative conditions. Cell Stem Cell 2015; 17: 35–46. [PubMed: 26095048]
32. Ema H, Morita Y, Suda T. Heterogeneity and hierarchy of hematopoietic stem cells. Exp Hematol 2014; 42: 74–82.e2. [PubMed: 24269919]
33. Sager HB, Heidt T, Hulsmans M, et al. Targeting interleukin-1p reduces leukocyte production after acute myocardial infarction. Circulation 2015; 132: 1880–1890. [PubMed: 26358260]
34. Ueda Y, Cain DW, Kuraoka M, et al. IL-1R type I-dependent hemopoietic stem cell proliferation is necessary for inflammatory granulopoiesis and reactive neutrophilia. J Immunol 2009; 182: 6477–6484. [PubMed: 19414802]
35. Cani PD, Amar J, Iglesias MA, et al. Metabolic endotoxemia initiates obesity and insulin resistance. Diabetes 2007; 56: 1761–1772. [PubMed: 17456850]
36. Hotamisligil GS, Shargill NS, Spiegelman BM. Adipose expression of tumor necrosis factor-alpha: direct role in obesity-linked insulin resistance. Science 1993; 259: 87–91. [PubMed: 7678183]
37. Shoelson SE, Lee J, Goldfine AB. Inflammation and insulin resistance. J Clin Invest 2006; 116: 1793–1801. [PubMed: 16823477]
38. Weisberg SP, McCann D, Desai M, et al. Obesity is associated with macrophage accumulation in adipose tissue. J Clin Invest 2003; 112: 1796–1808. [PubMed: 14679176]
39. Kueh HY, Champhekar A, Nutt SL, et al. Positive feedback between PU.1 and the cell cycle controls myeloid differentiation. Science 2013; 341: 670–673. [PubMed: 23868921]
40. Nerlov C, Graf T. PU.1 induces myeloid lineage commitment in multipotent hematopoietic progenitors. Genes Dev 1998; 12: 2403–2412. [PubMed: 9694804]

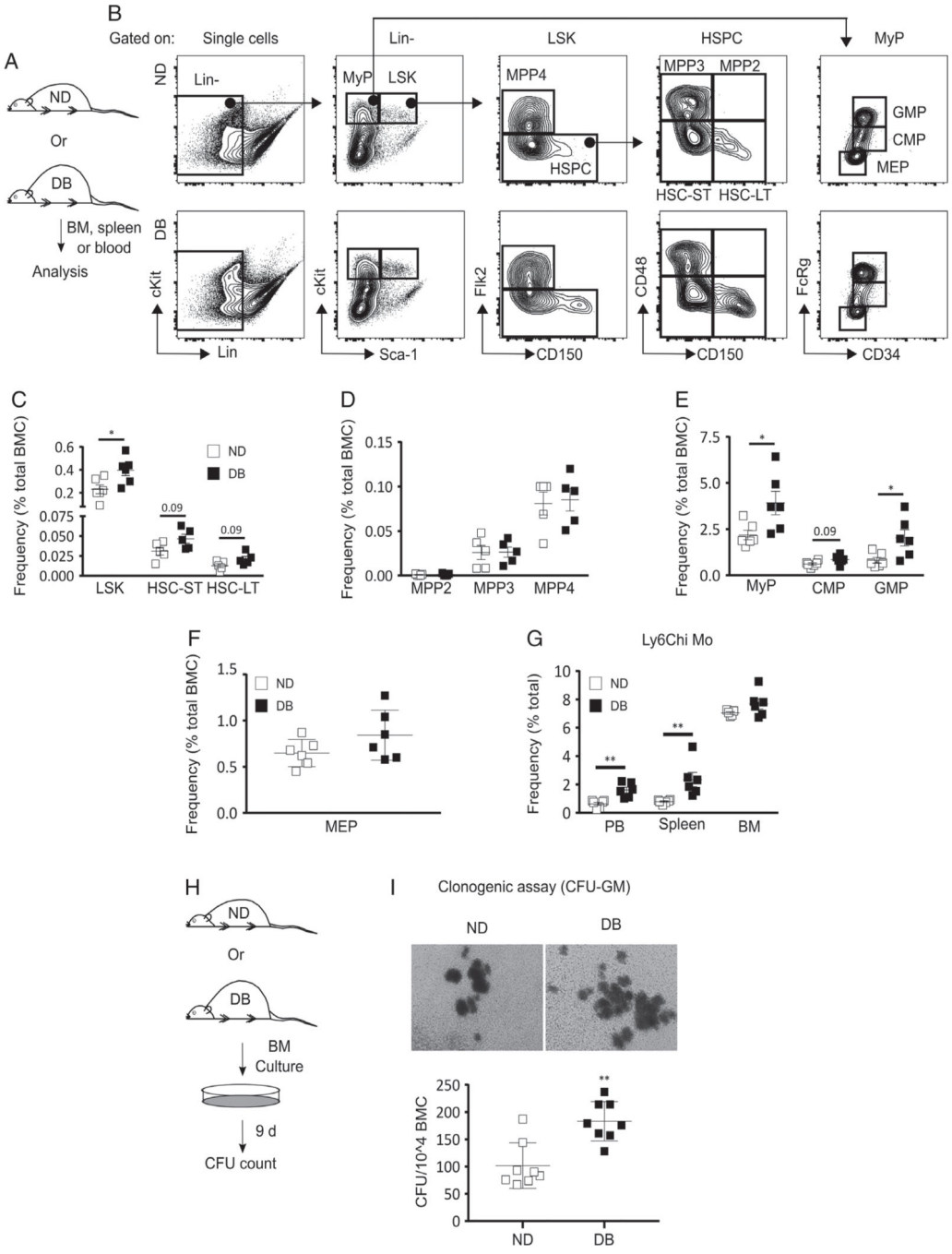

Figure 1.

T2D preprograms HSPCs towards myeloid differentiation at baseline. (A) Experimental design. (B) Representative flow cytograms showing the gating strategy for flow cytometry analysis of HSPC and MyP subsets in the BM of DB and ND mice. Percentage [of total BM cells (BMC)] of (C) LSK ($Lin^{-}Sca\text{-}1^{+}cKit^{+}$), HSC-ST ($Lin^{-}Sca\text{-}1^{+}cKit^{+}Flk2^{-}CD48^{-}CD150^{-}$), and HSC-LT ($Lin^{-}Sca\text{-}1^{+}cKit^{+}Flk2^{-}CD48^{-}CD150^{+}$); (D) MPP2 ($Lin^{-}Sca\text{-}1^{+}cKit^{+}Flk^{-}CD150^{+}CD48^{+}$), MPP3 ($Lin^{-}Sca\text{-}1^{+}cKit^{+}Flk^{-}CD150^{-}CD48^{+}$), and MPP4 ($Lin^{-}Sca\text{-}1^{+}cKit^{+}Flk^{-}CD150^{-}$); (E) MyP ($Lin^{-}Sca\text{-}1^{-}cKit^{+}$), CMP ($Lin^{-}Sca\text{-}1^{-}cKit$

$^{+}$FcRγloCD34^{+}), and GMP (Lin^{-}Sca-1^{-}cKit^{+}FcRγhiCD34^{+}); and (F) MEP (Lin^{-}Sca-1^{-}cKit^{+}FcRγloCD34^{-}) in DB and ND BM. (G) Percentage (of total cells) of Ly6Chi Mo (Ly6G^{-}CD11b^{+}Ly6Chi) in BM, peripheral blood (PB), and spleen of DB and ND mice. (H, I) Clonogenic assay: (H) experimental design and (I) representative culture photographs (upper panel) and number of colony-forming units (CFU) per 10^4 BMC (lower panel) in BM culture from DB and ND mice. Mean±SD, n=5–6 (A–G) and 4 mice in duplicate (H, I) for each strain. Data were compared between DB and ND groups using the Mann–Whitney U-test. Differences between groups were considered significant if $p \leq 0.05$. $^{*}p \leq 0.05$; $^{**}p \leq 0.01$.

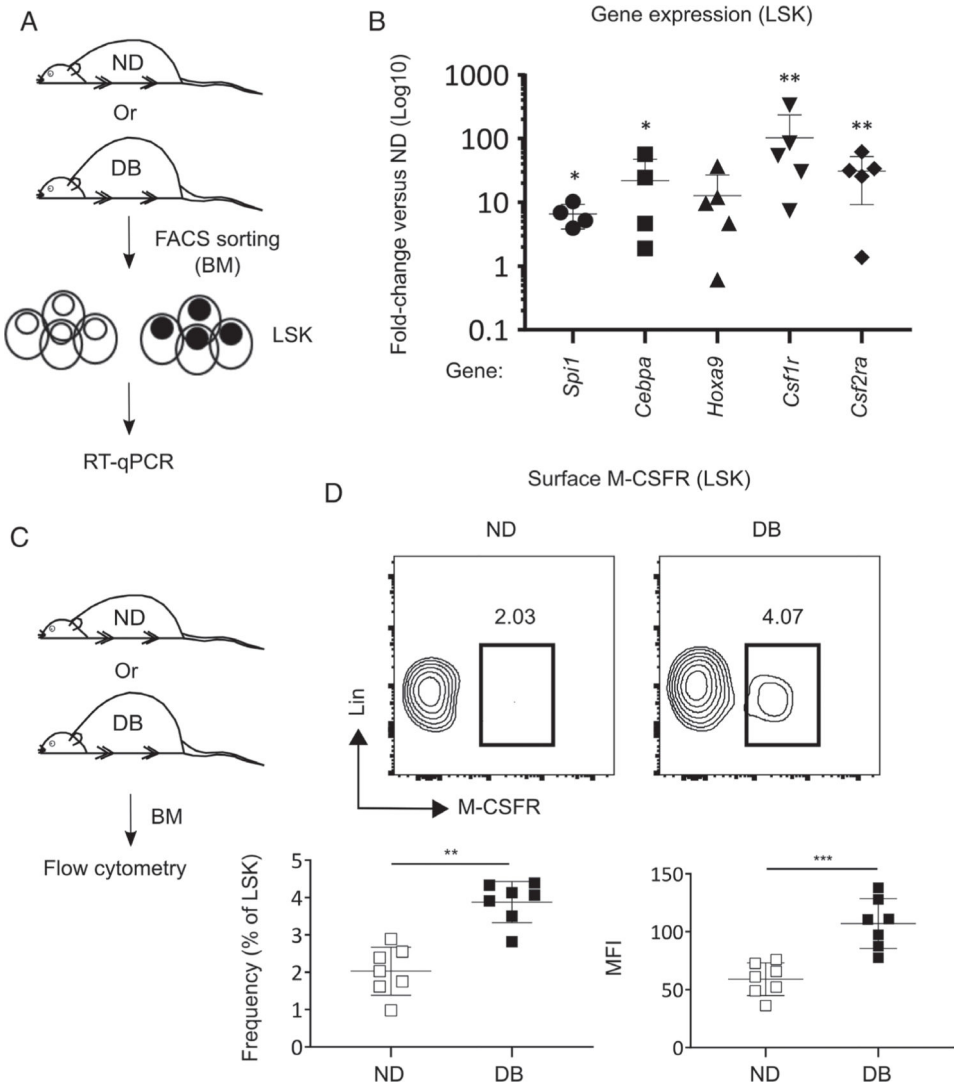

Figure 2.

BM LSK cells in DB mice are intrinsically modified towards myeloid lineage commitment. (A, B) Gene expression in LSK cells: (A) experimental design and (B) RT-qPCR for mRNA expression for transcription factors and surface receptors associated with myeloid commitment in LSK cells isolated from DB and ND BM. Data shown as relative fold-change of mRNA transcript in DB mice as compared with ND controls. (C, D) Surface M-CSFR protein: (C) experimental design and (D) representative flow cytograms (upper panel) and percentage (of LSK cells) and mean fluorescence intensity (MFI) of M-CSFR on LSK cells in DB and ND BM. Mean ± SD, n=4–5 (A, B) and 7 (C, D) mice for each strain. One sample was excluded from statistical analysis for *Spi1* and *Cebpa* mRNA expression (in B) because of very high PCR cycle numbers and thus we considered this data point an outlier. Data were compared between DB and ND groups using a Mann–Whitney U-test. Differences between groups were considered significant if $p \leq 0.05$. $^{*}p \leq 0.05$; $^{**}p \leq 0.01$; $^{***}p < 0.001$.

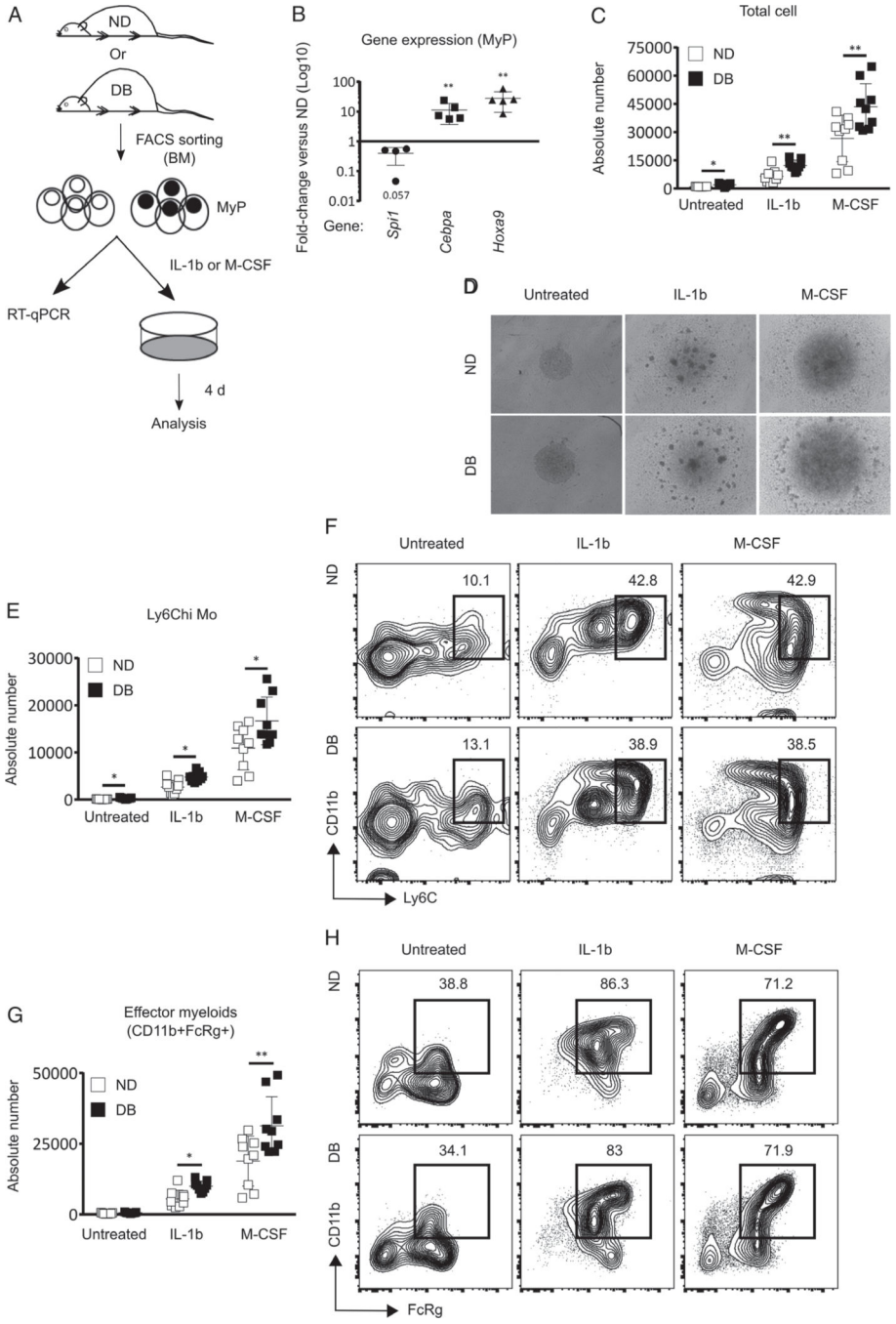

Figure 3.

T2D primes MyP to promote myelopoiesis *ex vivo.* (A, B) Gene expression in MyP: (A) experimental design and (B) RT-qPCR for relative mRNA expression of myeloid differentiation-associated transcription factors in MyP from DB and ND BM. (C–H) MyP liquid culture: (C) absolute number of total cells, (D) representative photographs of MyP cultures, (E) absolute number of Ly6Chi Mo ($CD11b^{+}Ly6Chi$), (F) representative flow cytograms showing mean percentages of Ly6Chi Mo, (G) absolute number of effector myeloid cells ($CD11b^{+}FcR\gamma^{+}$), and (H) representative flow cytograms showing mean

percentages of effector myeloids in MyP cultures from DB and ND mice in the presence or absence of IL-1β (5 ng/ml) and M-CSF (25 ng/ml). Data are shown as relative fold-change in mRNA levels in DB mice as compared with ND controls. Mean ± SD, n=4–5 mice for each strain (B) and three independent experiments in triplicate (C–H). One sample was excluded from statistical analysis for *Spi1* mRNA expression (in B) because of very high PCR cycle numbers and thus we considered this data point an outlier. Data were compared between DB and ND groups using a Mann–Whitney U-test. Differences between groups were considered significant if $p < 0.05$. *$p < 0.05$; **$p < 0.01$.

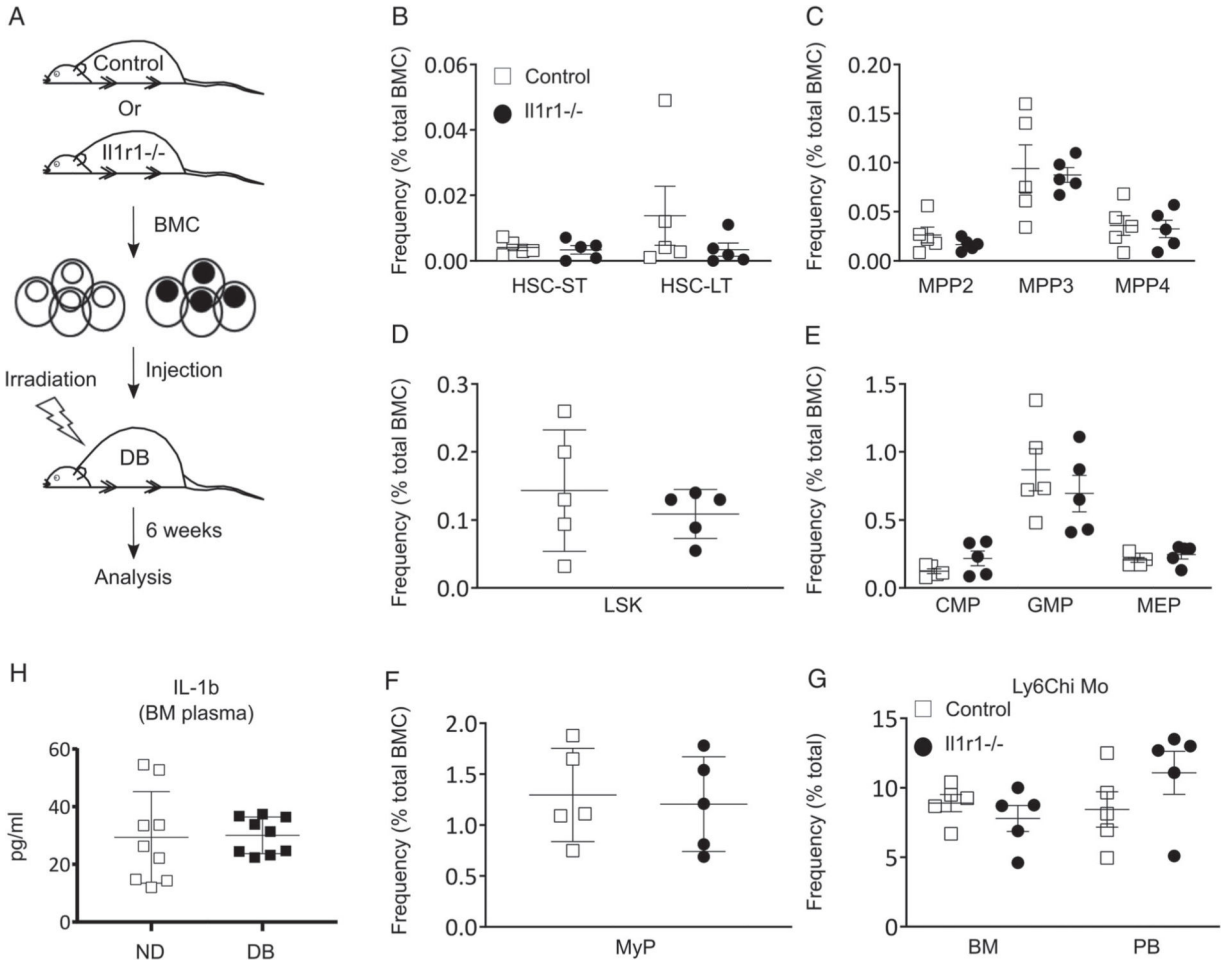

Figure 4.

IL-1R1 signaling likely does not influence myeloid commitment in DB mice. (A) Experimental design; (B) percentage (of total BMC) of HSC-ST and HSC-LT; (C) MPP2, MPP3, and MPP4; (D) LSK; (E) CMP, GMP, and MEP, and (F) MyP in the BM; and (G) Ly6Chi Mo in the BM and PB of DB recipient mice 6weeks post-transplantation with $Il1r1^{-/-}$ or C57BL/6 WT control BM cells. (H) Level of IL-1β protein in BM plasma of DB and ND mice as measured by ELISA. Mean±SD, n=5 mice per group (A–G), and 9 mice for each time point for each strain (H). Data were compared between groups using a Mann–Whitney U-test. Differences between groups were considered significant if $p \leq 0.05$.

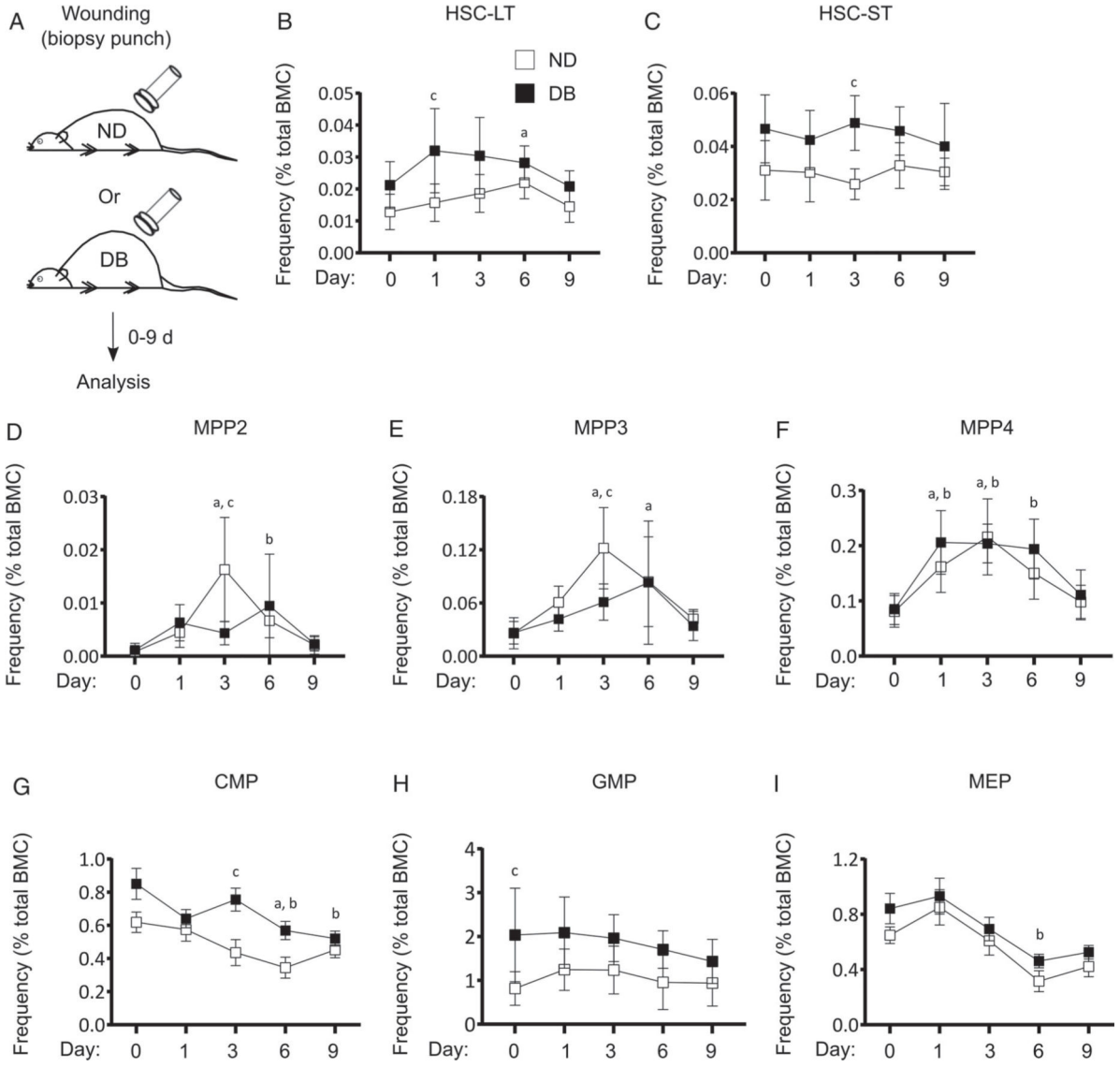

Figure 5.

T2D alters HSPC response to skin wounding in DB mice. (A) Experimental design, (B) percentage (of total BMC) of HSC-LT, (C) HSC-ST, (D) MPP2, (E) MPP3, (F) MPP4, (G) CMP, (H) GMP, and (I) MEP in the BM of DB and ND mice at different time points post-skin wounding. Mean±SD, n=5–6 mice for each time point for each strain. Data were compared between DB and ND groups over different time points using two-way ANOVA and over different time points in the same group using one-way ANOVA (Kruskal–Wallis test) in kinetic assays. Differences between groups were considered significant if $p \leq 0.05$. a, mean value significantly different from day 0 in ND; b, mean value significantly different from day 0 in DB; c, mean value significantly different between two strains at the same time point.

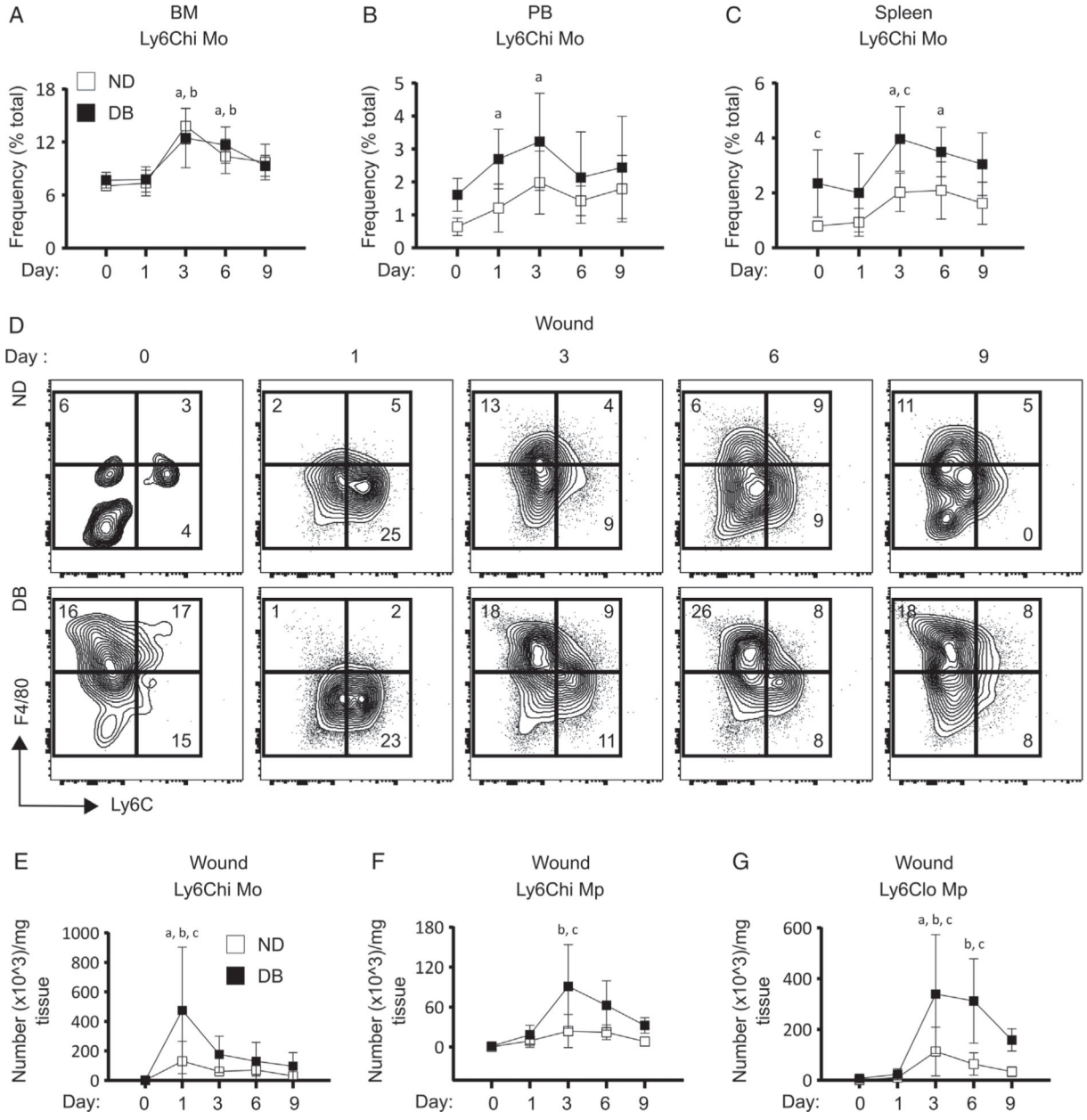

Figure 6.

T2D increases Ly6Chi Mo numbers in the circulation and spleen and Mo/Mp in the wounds of DB mice following skin wounding. (A–C) BM, circulating and splenic Ly6Chi Mo; (A) percentage (of total cells) of Ly6Chi Mo in BM, (B) PB and (C) spleen of DB and ND mice at different time points following skin wounding. (D–G) Wound Mo/Mp; (D) representative flow cytograms with mean percentages, and absolute numbers of (E) Ly6Chi Mo, (F) Ly6Chi Mp, and (G) Ly6Clo Mp in the wounds of DB and ND mice at different time points post-skin wounding. Mean±SD, n=5–6 mice for each time point for each strain. Data were compared between DB and ND groups over different time points using two-way ANOVA and over different time points in the same group using one-way ANOVA (Kruskal–Wallis test) in kinetic assays. Differences between groups were considered significant if $p \leq 0.05$. a,

mean value significantly different from day 0 in ND; b, mean value significantly different from day 0 in DB; c, mean value significantly different between two strains at the same time point.